THEORETICAL VELOCITY PATTERNS IN ICE COVERED STREAM CHANNELS

S. P. Chee
Department of Civil Engineering
University of Windsor
Windsor, Ontario
Canada
N9B 3P4

and

M. R. Haggag
L. P. Meyer and Associates
Windsor, Ontario
Canada

SYNOPSIS

A mathematical model was developed to predict the velocity pattern in ice covered channels. Initially, it involves the solution of the Reynolds' form of the Navier-Stokes equation in two-dimensional flow. The solution of these velocity profiles is applied to vertical and horizontal finite strips of the cross-section to obtain two sets of equations. These two solutions are combined through a coefficient equation and in conjunction with further hydraulic relationships, the flow pattern of three-dimensional ice-covered channels are derived.

INTRODUCTION

It is well known that the presence of an ice cover in a stream channel presents numerous hydraulic problems such as ice jams, high upstream water elevations causing flooding, reduced conveyance capacity and others. Central to the solution of these problems is a knowledge of the velocity pattern of the river channel. The boundary roughnesses and the configuration of the cross-section are very important parameters that determine the velocity profile. Owing to the irregular shape of channel cross-sections in nature as well as its varying roughnesses, the solution to this becomes very complex. In this paper, a mathematical model, which incorporated these parameters, was employed to obtain a comprehensive solution.

THEORETICAL ANALYSIS

Problem Definition

The flow pattern problem can be defined by the following statement. For an ice-covered channel of known cross-sectional shape and boundary roughness, the flow pattern can be determined once either the flowrate or energy slope is given. The flow is taken as quasi-steady and quasi-uniform.

The complete solution to the problem lies in solving the general equation of motion, which is the Reynolds' form of the Navier-Stokes equation. This difficulty arises from the existence of a differential shear on the opposite faces of any flow element parallel to the direction along which the equation is integrated. If this differential shear disappears, the equation can be integrated and this represents the case of two-dimensional flow. This concept will be used to develop the velocity profile in a channel where cross-currents are assumed to be absent.

Three-Dimensional Problem

In Figure 1, vertical and horizontal strips of unit widths are defined at a particular point P within the cross-section. A two-dimensional solution to determine the velocity profile for the vertical strip is undertaken on the assumption that this strip represents a part of a wide channel where it would be justified to neglect the horizontal shear. The local depth is denoted by Y_p and roughnesses by n_1, n_2, and the vertical shape function of the local relative velocity by $(U/V)_y$. A similar solution conducted for the horizontal strip using its local width Z_p and roughnesses n_3 and n_4 to yield the transverse shape function of the local relative velocity $(U/V)_z$, in which (U/V) is the ratio between the velocity at point P and the mean velocity at each strip.

The relative velocity at the point P can be determined if these two solutions are used as coefficients of each other through a coefficient equation. The successive application of the equation at every point with the channel cross-section will provide the complete determination of the velocity profile in the channel.

Two Dimensional Determination of Velocity Profile

The general Reynolds' form of the Navier-Stokes equation in two dimensional flow can be written for the vertical strip as

$$\bar{U}(\partial\bar{U}/\partial x) + \bar{V}(\partial\bar{U}/\partial y) + \partial\overline{U'U'}/\partial x + \partial\overline{V'U'}/\partial y =$$

$$[1] \qquad -\frac{\partial}{\partial x}(\bar{P}/\rho + gh) + \frac{\mu}{\rho}\left(\frac{\partial^2\bar{U}}{\partial x^2} + \frac{\partial^2\bar{U}}{\partial y^2}\right)$$

in which $\bar{U}$, $\bar{V}$, are the average velocities in the x and y directions, U', V' are the variations in the $\bar{U}$ and $\bar{V}$ values, ρ and μ are the fluid density and viscosity, and $\bar{P}$ = average pressure. For gravity, as well as a steady and uniform flow with no cross-currents, Equation 1 becomes

$$[2] \qquad \frac{\partial}{\partial y}\left(\mu\frac{\partial\bar{U}}{\partial y} - \rho\overline{U'V'}\right) = -\rho\, g\, S$$

where S is the bed slope and g is the acceleration due to gravity. The laminar shear is denoted by the first term in Equation 2 while the second quantity represents the turbulent shear.

The integration of Equation 2 for each subsection on its own, noting that the shear vanishes at the separation line, yields the shear distribution,

$$[3] \qquad \tau_{ti} + \tau_{Li} = \rho\, g\, S\,(Y_i - y_i) \qquad ,i = 1,2$$

in which the turbulent shear is denoted by τ_{ti}, the laminar shear is τ_{Li}, Y_i = distance

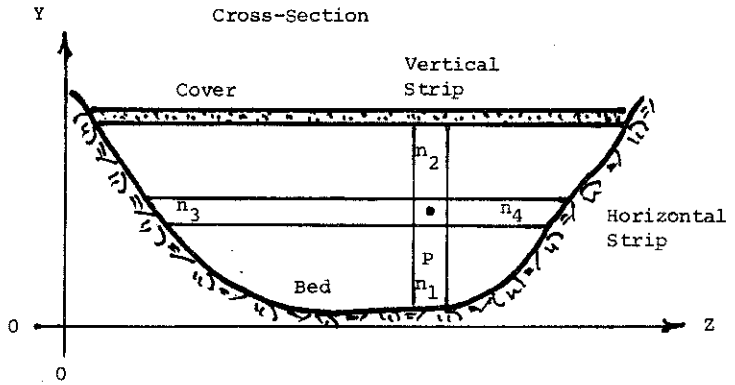

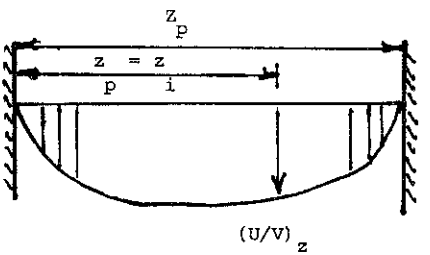

Horizontal Velocity Distribution

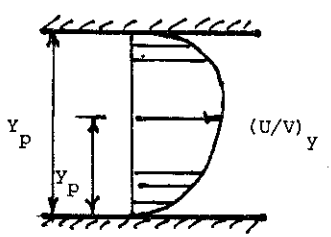

Vertical Velocity Distribution

Figure 1: General Technique for Velocity Profile Determination

from the bed or ice cover to the division line, y_i is the distance measured from the bed or the cover; and the subscript i = 1,2, refers to the bed and cover subsections respectively. The definition diagram is given in Figure 2.

The laminar shear is very small outside the laminar sublayer, hence, only the turbulent shear is retained. Within the turbulent core, the shear distribution can be respresented by the equation,

$$\tau_{ti} = \rho\, g\, S\, (Y_i - y_i) \qquad ,i = 1,2 \tag{4}$$

Using the Prandtl-Karman mixing length theory, the turbulent shear can be expressed as

$$\tau_{ti} = \rho\, y_i^2\, \kappa^2\, (dU_i/dy_i)\, |\, (dU_i/dy_i)\, | \qquad ,i = 1,2 \tag{5}$$

where κ is Von Karman's constant. Combining the previous equations, noting that $\varepsilon_i = y_i/Y_i$ = the relative depth, results in

$$dU_i/d\varepsilon_i = (V_{*i}/\kappa)\, \sqrt{1 - \varepsilon_i}\, /\, \varepsilon_i \qquad ,i = 1,2 \tag{6}$$

where V_{*i} = shear velocity = $\sqrt{g\, Y_i\, S_o}$.

The integration of this equation yields

$$U_i(\varepsilon_i) = (V_{*i}/\kappa)\, F'\, (\varepsilon_i) + C_i \qquad ,i = 1,2 \tag{7}$$

where $F'\, (\varepsilon_i)$ is given as

$$F'(\varepsilon_i) = 2\, \sqrt{1 - \varepsilon_i} - \mathrm{Ln}\, \frac{1 + \sqrt{1 - \varepsilon_i}}{1 - \sqrt{1 - \varepsilon_i}} \qquad ,i = 1,2 \tag{8}$$

The velocity profile should satisfy two boundary conditions:

1. The computed mean velocities should equal the existing one, i.e.

$$(1/A) \int U_i(y_i)\, dy_i = V_i \qquad ,i = 1,2 \tag{9}$$

hence, the integration constant C_i is

$$C_i = V_i + 2\, V_{*i}/\, 3\kappa \qquad ,i = 1,2 \tag{10}$$

2. At the point of separation, $\varepsilon = 1$, the velocity is maximum, and C_i should be

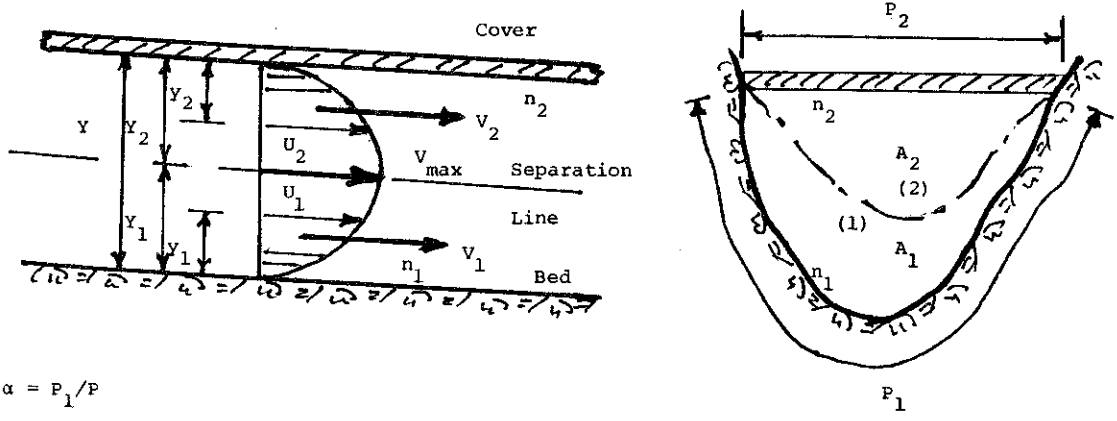

$$\alpha = P_1/P$$

$$\lambda = R_2/R_1 = \frac{A_2/P_2}{A_1/P_1}$$

Figure 2: Definition Sketch

[11] $$C_i = V_{max} \qquad ,i = 1,2$$

The velocity profile can then be defined by the following two equations:

[12] $$V_i - U_i(\varepsilon_i) = V_{*i}\, F_1(\varepsilon_i) \qquad ,i = 1,2$$

and

[13] $$V_{max} - U_i(\varepsilon_i) = V_{*i}\, F_2(\varepsilon_i) \qquad ,i = 1,2$$

and their values are respectively

[14a] $$F_1(\varepsilon_i) = \frac{2}{\kappa}\left(\mathrm{Ln}\left(\sqrt{\varepsilon_i}/\left(1 - \sqrt{1 - \varepsilon_i}\right)\right)\right) - \sqrt{1 - \varepsilon_i} - 1/3 \qquad ,i = 1,2$$

and

[14b] $$F_2(\varepsilon_i) = \frac{1}{\kappa}\left(\mathrm{Ln}\,\frac{1 + \sqrt{1 - \varepsilon_i}}{1 - \sqrt{1 - \varepsilon_i}} - 2\sqrt{1 - \varepsilon_i}\right)$$

and the maximum velocity is related to the mean velocities in the form

[15] $$V_i = V_{max} - 2\, V_{*i}/\, 3\kappa \qquad ,i = 1,2$$

To use the developed velocity profile, the position of the maximum velocity, i.e. Y_1 and Y_2, should be estimated. These values depend upon the roughness of each boundary and the depth.

Similar relations can be developed for the horizontal strip with the substitution of

[16] $$\varepsilon_i = z_i / Z_i \qquad ,i = 1,2$$

where z_i and Z_i are defined in Figure 1.

General Solution

The velocity profile can be obtained by combining all the previously derived equations with the coefficient equation. The solution can only be performed numerically.

DISCUSSION OF RESULTS

Two-Dimensional Case

The difference between the two subsection mean velocities can be written as,

$$[17] \qquad V_1 - V_2 = \frac{-2}{3\kappa} (V_{*1} - V_{*2})$$

and hence the rougher the boundary the smaller its subsection velocity. In fact the same applies to the mean and maximum velocities of the whole section. The ratio of these two velocities can be evaluated as

$$[18] \qquad \frac{V_{max}}{V} = 1 + \frac{2}{3\kappa} \left(\frac{V_{*1}}{V} \frac{A_2}{A} + \frac{V_{*2}}{V} \frac{A_1}{A}\right)$$

and the rougher the boundaries, the higher this ratio will be.

To test the applicability of the developed velocity profile, the velocities were measured at the center of the wide flume. The bottom Manning's roughness n_1 was .011 while the cover underside roughness n_2 was measured on a lined channel at .032. The measured flow rates were used to develop the theoretical velocity profiles and the results were compared to the measured velocities.

Good agreement between the theoretical and measured velocity profiles was obtained. The measured velocities were slightly greater than the predicted ones near the cover boundary, but this can be attributed to the release of the cover resistance due to the gap through which the Pitot-tube was introduced.

Most of the velocity profiles in the literature do not agree on the value of the computed velocity at and near the point of separation, where they have a discontinuous profile. To have a continuous profile, a maximum velocity has to occur at the separation point when computed from both sides. This does not appear to be the case when applying the direct logarithmic velocity profiles commonly used in the literature and reported by Uzuner (1975) on the work of Beloken (1938) and Levi (1948); Bolsegna (1968), Synotin (1965), Larsen (1966) Tesaker (1970) and others.

Three-Dimensional Velocity Pattern

The velocity profiles and composite roughnesses for different cross-sections were tested against these reported by Wong (1979) as shown in Figure 3. It can be seen from this comparison that the prediction is in good agreement with the measurements.

CONCLUSIONS

The theory developed in this paper showed promise in predicting the velocity patterns in three-dimensional ice-covered channels. From the experimental data of prismatic polygonal channels good agreement has been obtained. Comparisons of velocity patterns of ice-covered streams in nature are required to further confirm the theory.

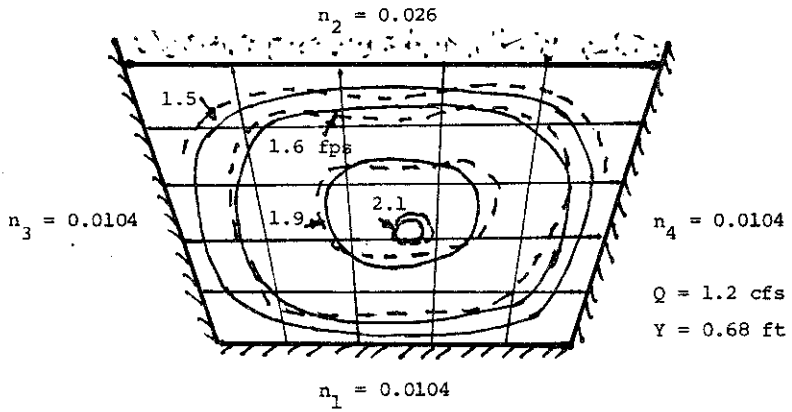

Figure 3a: Velocity Comparison for Trapezoidal Channel

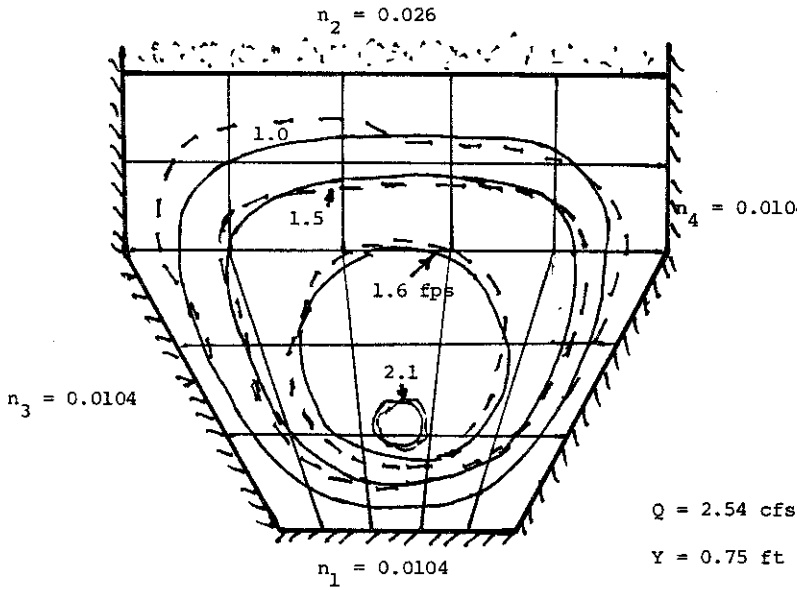

_____ Theory

---------- Experiment

Figure 3b: Velocity Comparison for Compound Trapezoidal Channel

ACKNOWLEDGEMENT

The research grant provided by the Natural Sciences and Engineering Research Council Canada is gratefully acknowledged.

REFERENCES

Bolsegna, S. J. 1968. River ice jams: State of the art report. U.S. Army, CRREL.

Larsen, P. A. 1966. Head losses caused by an ice cover on open channels. Boston Society of Civil Engineers, pp. 45-67.

Synotin, V. I. 1965. Velocity structure of flow under ice cover. I.A.H.R. Ice Symposium, Montreal.

Tesaker, E. 1970. Measurements of ice cover roughness and the effect of ice cover on water levels in three Norwegian rivers. I.A.H.R. Symposium on Ice, Reykjavik, Iceland.

Uzuner, M. S. 1975. The composite roughness of ice covered streams. I.A.H.R. Journal of Hydraulics, Vol. 3, No. 1, pp. 79-102.

Wong, Y. F. 1979. Hydraulics of covered channels. M.A.Sc. Thesis, University of Windsor, Windsor, Ontario.

DISCUSSION:

Gerry Beckstread, Hydrocon Engineering Ltd.

Figure 3 illustrates a comparison of laboratory and computed velocity profiles, for prismatic channels with equal roughnesses on the sides. Have any comparisons been made for channels that are non-prismatic and/or that have non-equal side roughnesses?

Reply by S.P. Chee and M.R. Haggag

No comparisons have been made for channels that are non-prismatic up to date; we intend to make these comparisons in the future. Experiments are currently in progress using prismatic channels with non-equal side roughnesses.

R. Gerard, University of Alberta

What advantages does your technique have over that used by Leighly in 1932 and Taylor in 1958?

Reply by S.P. Chee and M.R. Haggag

We have not read the papers by Leighly (1932) and, presumably, that of Deissler and Taylor in 1958 and, therefore, could not critically discuss the question. However, in general, our technique in theory could be used in rivers with multiple boundary roughnesses and could be extended to rivers in nature with and without ice covers.